soil systems

MDPI

Article

Formation of the Azodication (ABTS^{2+}) from ABTS [2,2′-Azinobis-(3-ethylbenzothiazoline-6-sulphonate)] in Sterile Plant Cultures: Root–Exuded Oxidoreductases Contribute to Rhizosphere Priming

Gerhard Gramss

Institute of Earth Sciences, Friedrich-Schiller-University, Burgweg 11, D-07749 Jena, Germany; gerhard.gramss@uni-jena.de

check for updates

Abstract: Rhizosphere priming by terrestrial plants comprises increased or repressed efflux of CO_2 and N from soil organic matter (SOM), decaying under the impact of temperature, moisture, and the composition of rhizodeposits. Contemporarily, increases in water solubility vs. losses in molecular size, aromaticity, and the content in phenolic OH groups denote the degradation of SOM in planted soil. Root peroxidases (POs) and 'polyphenoloxidases' are surmised to contribute to these effects, however, final evidence for this is lacking. Therefore, seedlings of white mustard, alfalfa, and oilseed rape with wide spans in PO release were grown in hydroponic cultures at variable levels of Cu/Fe/Mn as Fenton metals, but also under P and Fe starvation to stimulate the release of carboxylic acids that form catalytic Mn^{3+} chelants from Mn^{2+} and MnO_2. The shortage in active oxygen as a cosubstrate of POs delayed the immediate oxidation of 2,2′-azinobis-(3-ethylbenzothiazoline-6-sulphonate) (ABTS) supplements to the green ABTS$^{•+}$ by PO/H_2O_2, the possible formation of Mn^{3+} via PO catalyzed aryloxy radicals from root–released phenolics, and of HO$^{•}$ by metal cations in H_2O_2 dependent Fenton–like reactions. Enhanced by exuded and external malate, O_2 independent MnO_2 supplements in some treatments formed ABTS$^{•+}$ spontaneously. The culture fluids then turned red in all treatments within 24–60 h by the formation of azodication (ABTS^{2+}) derivatives in a second plant initiated oxidation step that is known to be catalyzed by substrate radicals. It is concluded that plants initiate oxidative activities that contribute to rhizosphere priming in an environment of oxidoreductase and carboxylate exudates, the indicated presence of mediating substrate radicals, and the cations and (hydr)oxides of transition metals. Pathways of H_2O_2 production upon the degradation of carboxylates and by the POs themselves are indicated.

Keywords: rhizosphere priming; humic substances; plant peroxidase; carboxylates; active oxygen; transition metals; Fenton–like reactions; ABTS cation radical; azodication derivatives

1. Introduction

Soil organic matter with an estimated amount of 1.6×10^{18} g C [1] is a major player in the terrestrial carbon cycle. Its formation from plant residues by soil fauna and microbiota is overlaid from the rhizosphere priming effect [2]. Poorly defined rhizosphere factors of herbs inhibit [3,4], but mainly stimulate, the mineralization of C (by 27–245%) and N compounds (by 36–62%) [5–7] to accelerate the biotic degradation of arable land [8].

Part of soil formation processes is the degradation of the recalcitrant aromatic structures of lignin and humic substances (HS). It is catalyzed by the joint action of dehydrogenases, oxygenases and oxidoreductases such as the laccases and peroxidases of plants, white–rot, soft–rot, brown–rot fungi and bacteria [9–12]. The enzymes operate in concert with low–molecular weight (MW) carboxylic acids,

(reactive) oxygen species, transition metal cations, and small organic radical molecules of substrate or metabolic origin with redox mediator properties [13–16]. They mediate electron abstractions from substrates whose electron withholding capacity (E^0) surpasses the redox potential of the enzyme itself.

Initial one–electron oxidations of the dominating non-phenolic lignin units presuppose redox potentials of $E^0 > 1.5$ V taken vs. normal hydrogen electrodes (NHE) [17]. This catalytic potential is afforded by lignin peroxidases and versatile peroxidases of certain wood-decaying basidiomycete fungi ($E^0 = 1.4$–1.5 V). The enzymes use H_2O_2 as an electron acceptor, see [9,15,18–20] for reviews. Manganese dependent peroxidases of basidiomycetous wood-decay and ground fungi complete their redox cycle by the oxidation of two Mn^{2+} cations to the abiotic oxidant Mn^{3+} ($E^0 = 0.8$–0.9 V for Mn^{3+}/malonate or oxalate complexes) [20,21]. The cation performs one-electron abstractions (H^+/e^-) from phenolic substrate molecules or phenolic lignin structures [22,23] upon its reduction to Mn^{2+}. It is enzymatically reoxidized to Mn^{3+} by electron transfer to H_2O_2. Laccases of basidiomycetes (E^0 up to 0.79 V) catalyze one-electron abstractions from hydroxyl groups of four phenolic molecules (up to 0.81 V) [24] to convert the electron acceptor O_2 to 2 H_2O. They initiate oxidations, decarboxylations, demethylations, and demethoxylations from phenolic acids (derivatives) and phenolic lignin moieties. Resulting aryloxy radicals polymerize or depolymerize to low-MW mediators to initiate spontaneous C_α-C_β bond cleavages, C_α oxidations, and alkyl-aryl and aromatic ring cleavages in phenolic lignin model compounds [25,26]. Laccase/synthetic mediator systems (E^0 up to 1.5 V) oxidize the lignin model surrogate veratryl alcohol ($E^0 = 1.4$ V) and nonphenolic structures of lignin model compounds [27–29].

The Mn-independent class (iii) plant peroxidases (PO; EC 1.11.1.7) have comparable substrate spectra as actors in rhizosphere priming. Their redox potential of $E^0 = 0.89$–0.95 V [18] surpasses that of fungal laccases and especially of plant laccases ($E^0 = 0.4$ V) and monophenol monooxygenases (MMO, EC 1.14.18.1, $E^0 = 0.26$ V) [15,30]. Plant POs catalyze one-electron oxidations of phenolics and humic substances [31] using H_2O_2 as electron acceptor according to the redox cycle.

$$\text{Two phenolic molecules} + H_2O_2 \rightarrow \text{Two aryloxy radicals} + \text{two } H_2O \qquad (1)$$

Plant released phenolics acting as aryloxy radicals mediate the formation of Mn^{3+} (0.8–0.9 V) [15,32] and a partial oxidation of veratryl alcohol from maize roots (1.4 V) [30]. They expand the substrate range at least in part to that of fungal POs.

In several plant tissues, more than 30 PO and several MMO [33] and laccase isoforms [34] can be found. In plant roots, the bulk of the PO is localized in the primary cell wall but also in membranes, organelles, vacuoles, and the cytoplasm [33]. Class (iii) peroxidases could thus be leached from roots of cotton, wheat, cress, tomato, water hyacinth, French bean, rice [33,35] and other plants [15,30,36]. Taken with the chromogen guaiacol at pH 7.0, alfalfa plants but not oilseed rape surpassed the root exuded PO activities of white mustard 167–182 times both in axenic and natural soil cultures [15,37]. Contemporarily, sterile root effluents of herbs contained little, if any, H_2O_2, or its precursor $O_2^{\bullet-}$, as the co-substrates of PO. Soil-grown alfalfa plants (40 d old) contained 42 mg kg^{-1} DW of peroxide in the shoot, and traces in root tissue and in aseptic root exudates [38].

With its content of up to 30% phenolic units [39], the humus polymer matches with the substrate spectrum of laccases, peroxidases, and abiotically generated oxidants such as hydroxyl radical (HO$^\bullet$) that is reduced to water upon H^+/e^- abstractions from organics ($E^0 = 1.8$–2.7 V) [40]. According to Haber and Weiss [41], HO$^\bullet$ as the ultimate oxidant is presumably formed by multivalent transition metals (M) such as Ce, Co, Cr, Cu, Fe, La, Mn, Ni, Ru, V, and others. They serve as electron donors upon H_2O_2 consume in a Fenton-like reaction [42–44]. Clay and oxide minerals such as MnO_2 can also serve as catalysts in Fenton-like reactions [45].

$$(M^n)^+ + H_2O_2 \rightarrow (M^{n+1})^+ + HO^\bullet + HO^- \qquad (2)$$

Soil humic substances (HS) and their alkali-extractable humic acids (HA, apparent molecular size 10–>300 kDa) and fulvic acids (FA, 0.1–9 kDa) are predominantly formed, and immediately released,

from senescent plant tissues [46]. Humic acids are mainly composed of (C-substituted) aromatics and alkyl-C (aliphatic structures) whereas fulvic acids represent randomly composed polysaccharides and little aromatics [47,48]. Their reactive dissociable groups are mainly carboxyl (-COOH), phenolic, enolic, and alcoholic hydroxyl (-OH), methoxyl (-OCH$_3$), sulphydryl (-SH), amino (-NH$_2$), and imino (=NH) type. Their protons (H$^+$) are exchangeable with metal cations and are preferred targets of oxidative enzymes [49–51]. The mean molecular size and the degree of aromaticity of soil derived HS were reduced by the fungal manganese peroxidase/Mn^{3+} couple, by the Mn-independent plant peroxidase, and the abiotic oxidants H$_2$O$_2$ and Mn(III)acetate *in vitro*. The hydrolytic β-glucosidase caused discoloration. Fungal tyrosinases and laccases had little, if any, effect [31]. Beside active catalysts as above, those of whole fungal and bacterial cultures, too, greatly reduced the chemical reactivity of soil HS to tetrazotized *o*-dianisidine [31]. This indicator of hydroxylated aromatics [52] reveals the oxidative depletion of OH groups by apparent H$^+$/e$^-$ abstractions.

The immediate impact of root released POs on soil forming processes evokes little attention. Their ecological role is poorly understood [15]. It is suggested that the presence of POs and MMOs released by potted herbs and soil microbiota could add to an accelerated efflux of nitrogen upon an expected oxidative degradation of their HS matrices [7,53]. Wood-decay fungi growing on sterile, HS amended media released MMOs, laccases, and manganese peroxidases. Within three weeks, the concentrations of HS decreased by 29–54%, their molecular size by 53–59%, and the loss in hydroxyl groups (-OH) amounted 89–99.6%. This indicated shifts to the aromatic-poor fulvic-acids pool [31] and mineralization by the MnP/Mn^{3+} system [54]. A natural forest soil C$_{org}$ 15–20% incubated with a set of plants for 56 d contained POs beside traces of laccase and MMO. Relative to unplanted controls and without H$_2$O$_2$ amendments, the water solubility of HS rose to 115–156%. The concentrations of their phenolic OH groups dropped by 53–79% (r = 0.815, $p \geq 0.67$) in PO releasing plants, and by 28–34% in plants with no extractable PO exudates, to copy the reactions obtained in fungal cultures [37].

The evidence for an apparent contribution of plant released oxidoreductases to rhizosphere priming as above is nevertheless indirect. In the present study, seedlings of the strategy-I plants white mustard, alfalfa, and oilseed rape were therefore cultivated in sterile hydroponic cultures by exclusion of enzyme releasing microorganisms. The plants were grown at variable levels of Fe and Mn as Fenton metals with potential HO$^\bullet$ generation. In addition, Fe and P starvation was observed to promote the release of carboxylic acids that form with Mn^{3+} chelates from MnO$_2$ supplements another abiotic catalyst [55]. The grown-up seedlings were amended with the susceptible and colorless chromogen 2,2′-azinobis-(3-ethylbenzothiazoline-6-sulphonate) (ABTS). It turns green upon its one-electron oxidation to the cation radical ABTS$^{\bullet+}$ (E^0 = 0.68 V), and red after a second oxidation step from ABTS$^{\bullet+}$ to the azodication ABTS^{2+} (ABTS$^{\bullet+}$ to ABTS^{2+}, E^0 = 1.09 V) (Figure 1) [56]. In a second trial, Fenton metals acting as micronutrients were exposed to H$_2$O$_2$ or O$_2^{\bullet-}$. Their ability was tested to oxidize ABTS by the formation of hydroxyl radical (HO$^\bullet$) even at the physiological pH conditions of the plant cultures. The goal was to use the unambiguous color reactions of ABTS for the definitive proof of the joint, and almost inseparable, oxidative activities afforded:

- by released oxidoreductases of gnotobiotic plants in the absence of H$_2$O$_2$ or O$_2^{\bullet-}$ supplements,
- by contributions of transition metal cations in Fenton-like reactions with active oxygen species,
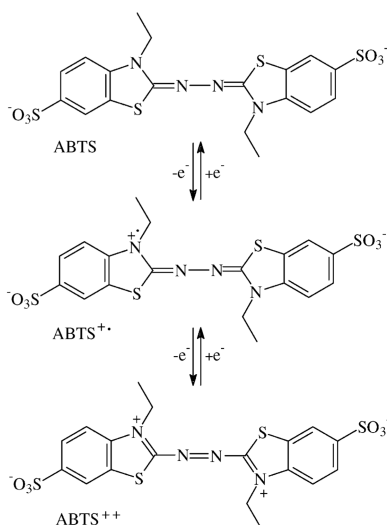- and by Mn^{3+} catalyst derived from MnO$_2$ by root-released and external malate.

Figure 1. Oxidation of the heterocyclic 2,2′-azinobis-(3-ethylbenzothiazoline-6-sulphonate) (ABTS) molecule (shown as a dianion) to $ABTS^{2+}$ by two consecutive electron abstractions.

2. Materials and Methods

2.1. Surface Sterilization of Seeds for Gnotobiotic Flask Cultures

Commercially available seeds (N. L. Chrestensen, Erfurt, Germany) were immersed in deionized water amended with the anionic detergent Fit (Fit GmbH, Zittau, Germany) for 2–6 h to remove adhering bubbles and make the kernels sink to the beaker's bottom. Those drifting above were removed. The remaining submerged seeds of white mustard (*Sinapis alba* L.) were surface-sterilized to 100% in 15% NaOCl (13% active chlorine) for 30 min and washed once in autoclaved water prior to the transfer into sterile 100-mL Erlenmeyer flasks for germination. The pre-submerged seeds of oilseed rape (*Brassica napus* L.) were surface-sterilized at a rate of around 67% in 30% NaOCl for 210 min and washed once prior to germination. Pre-submerged seeds of alfalfa (*Medicago sativa* L.) were surface-sterilized up to 100% in 30% H_2O_2 diluted to one-third for 20–30 min and used without washing. The treatment was accompanied by foam production incited by the kernels' surface peroxidase enzyme.

2.2. Hydroponic Flask Cultures

Cotton stoppered 100-mL Erlenmeyer flasks with 2.5 mL deionized water were autoclaved at 121 °C for 30 min. They were equipped with 1 cm^3 surface-sterilized seeds under air-controlled conditions, weighed, and incubated in the daylight at room temperature in a tilted position to avoid submergence of the kernels by the water resource. After 6–7 days, the emerging germlings were raised with a sterile nutrient solution adapted from Fries [57] and composed of (L^{-1}) 1 g KNO_3, 5 g KH_2PO_4, 0.01 g $CaCl_2$, 0.1 g NaCl, 0.01 g $FeSO_4 \cdot 7H_2O$, 2 mg $MnSO_4 \cdot H_2O$, 0.5 mg $ZnSO_4 \cdot H_2O$, and 0.5 mg $CuSO_4 \cdot 5H_2O$ (Merck, Darmstadt), pH 4.5. In the early growth stages, KH_2PO_4, $FeSO_4$ and/or $MnSO_4$ supplements were omitted. Within 3–4 weeks of incubation, the plants reached 45–65 mm (white mustard, oilseed rape) and 20–30 mm (alfalfa), respectively, in height and developed secondary leaves. At the outset of testing, the free liquid held at 2 mL was filled up to around 8.5 mL with the sterile nutrient solution modified in the P, Fe, and Mn content. Thereby, the mode of P or P/Fe(II) starvation was retained to increase the root exudation of malate/malonate [55]. Applications of Mn(II) were also withheld that could lead to the formation of the abiotic Mn^{3+} catalyst [58] by plant PO/root phenolic mediator systems [32,38]. Supplements of 50 mg autoclaved pyrolusite (MnO_2, Merck) in oxide activated or in the more passive powdered stage were used to serve as active-oxygen independent abiotic catalysts [45]. They could also serve as sources of Mn^{3+} liberated by root-exuded malate/malonate chelants or by external malate input [55]. The role of oxidoreductase

enzymes in ABTS transformations was illustrated with the application of *Pyricularia oryzae* laccase that, unlike plant PO, acts in the absence of active oxygen species such as $O_2^{\bullet-}$ and H_2O_2 and uses O_2 as electron acceptor [9,20]. Sterile-filtered high-performance liquid chromatography (HPLC)–grade ABTS (0.45 μm; Fluka) dissolved in a nutrient solution aliquot was applied one week later. The pH values of the resulting culture fluids rose from initial 4.4–4.7 to the later 5.1 in alfalfa and to 6.2 in white mustard. The final plant biomass ranged 0.38 to 0.5 g DW per flask. The sterility of the cultures was carefully supervised with the transfer of fluid aliquots to Standard I bacterial agar (Merck, Darmstadt).

2.3. Enzymatic and Chemical Tests

The activity of Mn-independent peroxidase (EC 1.11.1.7) in plant culture fluids war recorded as increase in A_{436} with 0.33 mL of the culture filtrate, 0.33 mL of 1.8 mM guaiacol, and 0.33 mL of 13.2 mM H_2O_2 prepared in 0.13 M potassium phosphate buffer pH 6.0 ($\varepsilon_{436} = 6400$ M^{-1} cm^{-1} for the resulting tetraguaiacol and other products) [59]. Enzyme reactions were followed at least in triplicate for 4 to 10 (to 30) min using UV-VIS spectrophotometry (Helios Beta, Unicam UV-VIS, Cambridge, UK). For the determination of plant laccase, H_2O_2 amendments were replaced by water. Monophenol monooxygenase (EC1.14.18.1) at pH 6.0 was measured as increase in A_{475} with 0.1 mL of culture filtrate and 0.9 mL of 15.6 mM DL-DOPA, 3,4-dihydroxyphenylalanine, prepared in 0.1 M potassium phosphate buffer ($\varepsilon_{475} = 3600$ M^{-1} cm^{-1} for the resulting dopachrome) [60].

For the qualitative detection of root released phenolics, culture fluid aliquots were boiled up for 10 s to inactivate enzymes. Then 1-mL aliquots were amended with 0.1 mL of a freshly prepared aqueous solution of 4.21 mM Fast Blue B salt (Acros). Increases in absorbance were recorded over the initial 10 s at 530 nm in quadruplicate and expressed as an increase in absorbance min^{-1} [52,61]. Peroxides in culture fluids were indicated with Merckoquant peroxide test strips (Merck). Non-oxidized remnants of ABTS in the fluids of plant cultures with azodication formation were determined in 1-mL reaction mixtures of 0.1 M potassium phosphate buffer pH 4.5 containing 0.1 mL of horseradish peroxidase (HRP, 0.3 mg 10 mL^{-1}; Merck) and 0.1 mL of the culture filtrate. The reaction was started with the application of 0.1 mL H_2O_2 (45 mg 10 mL^{-1}) and followed at A_{420}.

2.4. Oxidation of ABTS by Abiotic Catalysts

Triplicate samples of 4 mg from the transition metal compounds, $CoCl_2 \cdot 6H_2O$, $CuSO_4 \cdot 5H_2O$, $FeSO_4 \cdot 7H_2O$, $MnSO_4 \cdot H_2O$, and $Pb(CH_3CO_2)_2 \cdot 3H_2O$ (Merck) were weighed into 2 mL plastic microtubes. They were dissolved in 1.5 mL bideionized water or 0.15 M KH_2PO_4 buffer pH 4.5 and amended with 0.1 mL of aqueous 1.2 mM ABTS. Active oxygen species were added in the form of H_2O_2 (11 mg) and the superoxide anion radical ($O_2^{\bullet-}$) derived from 1.5–2 mg of the alkaline KO_2. The reaction mixtures were maintained in the physiological pH range of (2.3) 3.8 to >6.0 or acidified to pH 1.5–2 with H_2SO_4. UV-VIS spectrophotometry was used to quantify the formation of the green $ABTS^{\bullet+}$ solution at $\lambda = 420$ nm [59] and the red $ABTS^{2+}$ moieties by scanning spectrophotometry. The long-term presence of active oxygen was controlled with $O_2^{\bullet-}$ test strips (Merck).

2.5. Extraction of Aliphatic Carboxylic Acids for HPLC Examination

Carboxylic acids in culture fluids were extracted twice for 3 and 1 h, respectively, with 1.5 volumes of diethylether. Ether extracts were pooled and evaporated to a near-dryness (to prevent fatty acids from being blown out). Residues were resuspended in 1 mL of 0.005 M H_2SO_4 in bideionized water. Acids were quantified by HPLC using a Shimadzu SCL-10A model with a SPD-M10Avp diode array detector (Shimadzu Corp., Kyoto, Japan), and a Chrompack Organic acids column 300 × 6.5 mm (Varian Australia Pty Ltd., Mulgrave, Australia) under isocratic conditions. The mobile phase (0.6 mL min^{-1}) consisted of 0.005 M H_2SO_4 in bideionized water. Working conditions included 10 μL of sample injection, running time 20 min, column temperature 40 °C, and ultraviolet (UV) detection from 210 nm to 500 nm. Calibration (considering the losses to ether extraction) and establishment of a library to compare spectral profiles were performed with 23 individual HPLC-grade samples of mono-

to tricarboxylic acids (Merck). Several culture fluids were acidified with 0.2-% formic acid, centrifuged, and re-examined by HPLC (Agilent 1100; Agilent Technologies, Waldbronn, Germany) equipped with an Esquire 6000 ion-trap mass spectrometer (Bruker Daltonics, Bremen, Germany).

2.6. Actual Mineral Concentrations of White Mustard Culture Fluids

Appreciating the role of Cu, Fe, Mn, and P in the assays, aliquots of the final 8.5 mL of spent white mustard culture fluids were drawn from those five-week-old cultures that had not been amended with the respective minerals of interest (compare Section 2.2). The detected minor mineral pools were rated as seed-borne and liberated by leaching and root exudation. Samples of culture fluids were acidified to pH 2 with HNO_3, passed through 0.45 μm membrane filters, and analyzed by inductively coupled plasma mass spectrometry (ICP-MS; Thermo, X series).

2.7. Examination of $ABTS^{2+}$ Derivative by Liquid Chromatography

Non-purified culture fluid of the red $ABTS^{2+}$ derivative generated with white mustard was centrifuged at 14,000 g for 5 min, passed through a 0.45 μm membrane filter and analyzed by liquid chromatography with mass spectrometry detection (LC-MS) and pneumatically assisted atmospheric pressure ionization (API). The Perkin Elmer Sciex API 16 S with Series 200 pump and autosampler was run with 5.2 KV ionization voltage, 5 μL sample injection, and a flow of 0.25 mL min^{-1} under isocratic conditions. The eluent was composed of 10% methanol, 85% AFFA A, and 5% AFFA B.

AFFA A: 50 mM formic acid, 2 mM $NH_4^+HCOO^-$ in water.

AFFA B: 50 mM formic acid, 2 mM $NH_4^+HCOO^-$ in 95% acetonitrile.

2.8. Data Processing

In the case of numerical data, SPSS 8.0 software (Chicago, IL, USA) was used to calculate standard deviations (SD) of quadruplicate results, linear correlations, and to perform one-way analyses of variance. To determine the positions of the comparatively flat peaks obtained by spectrophotometric scans of ABTS solutions in the A_{340} to A_{800} range, absorbance values of the curves were determined for 5-nm intervals. Peaks were accepted where the differences between neighboring intervals dropped to zero. Most ABTS transformation data represent maximum values of four replicates.

3. Results and Discussion

3.1. Oxidation of ABTS by Gnotobiotic Plant Cultures

The three to four weeks old plants of the 100-mL microcosms raised aseptically in the absence of external P (from KH_2PO_4), Fe(II), or Mn(II) supplements had used seed internal resources to cover their mineral demand. They leached the Fenton metals Cu, Fe, and Mn at ppb amounts into the final 8.5 mL of free liquid (Table 1) to complicate interpretations of their role in the catalytic system by their ubiquitous background presence. Root released peroxidases converted guaiacol (mM min^{-1}, 20 °C) at 0.202 ± 0.069 in white mustard, at 0.376 ± 0.04 in oilseed rape, and at 11.23 ± 1.72 in alfalfa (n = 15). Traces of laccases and MMO were negligible. Active oxygen and root exudate of phenolics ranged below the detection limit. Concentrations (mg L^{-1}) of malate/malonate released by white mustard roots amounted zero in the presence of P and Fe supplements, 7.7 under P starvation, and 24 under P and Fe starvation. Both carboxylates were not found in cultures of oilseed rape and alfalfa.

With the contemporary exposure to the chromogenic ABTS and some of its potential oxidants, the plant cultures did not immediately form notable amounts of the green $ABTS^{•+}$ solutions absorbing at λ = 420 nm (A_{420}; Table 1). The apparent shortage in active oxygen species hid the minor oxidative activities of the root-released PO, the possible formation of Mn^{3+} oxidant by PO-catalyzed aryloxy radicals, or the production of $HO^•$ with the aid of Cu, Fe, and Mn cations in H_2O_2 dependent Fenton-like reactions [42]. However, not only laccase (treatment 4b, Table 1), the Mn(II)/Mn(IV) couple, too, oxidized ABTS spontaneously to the green cation radical. Thereby, the oxide activated

MnO_2 reached higher A_{420} values than its powdered surrogate, supported by malate supplements. The green solutions bleached within 7–30 h to gradually express red color tones after 24–60 h in all treatments of white mustard (1a–4b) and in oilseed rape. Alfalfa plants known to surpass root exuded PO activities of white mustard up to 167–182 times both in axenic and natural soil cultures [15,37] formed red derivatives peaking at A_{543} in a superior quantity without a notable phase of preceding A_{420} intermediates (Figure 2). The position of absorbance peaks in red culture fluids point to the presence of $ABTS^{2+}$ in the A_{515} to A_{520} range [56]. Modifications of the azo dication in solutions peak at A_{542} to A_{561} [62]. Heat-killed plant control cultures devoid of MnO_2 and PO activity did not oxidize ABTS.
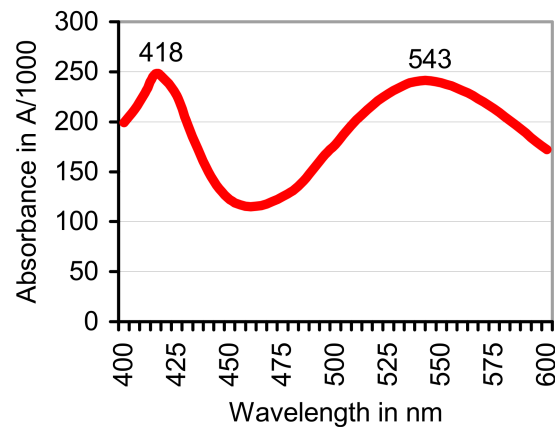

Figure 2. Spontaneous oxidation of ABTS to derivatives of the azodication $ABTS^{2+}$ absorbing at A_{543} in sterile hydroponic culture of alfalfa, supported by Cu, Fe, and Mn(II)/Mn(IV) amendments (refer to Table 1). The absorbance peak at 418 nm refers to non-converted $ABTS^{\bullet+}$ residues.

Upon the formation of the red derivatives, both active oxygen and PO proved to be the limiting factors. Adding H_2O_2 and HRP to culture fluid aliquots resulted in spontaneous and intense reddenings. This includes that root-derived phenolics converted to aryloxy radicals by PO/active oxygen and/or by Mn^{3+} must have been present in excess.

Table 1. Oxidation of ABTS to ABTS$^{\bullet+}$ (A_{420}, temporary maximum values) and ABTS^{2+} derivatives (A_{520} to $A_{561} \pm$ SD) by sterile hydroponic cultures of white mustard (treatments 1a to 4b), oilseed rape, and alfalfa in the alternating presence of phosphate and transition metals leached from seeds (maximum **Leach** values) or added up with the nutrient solution (sum, in mg L^{-1}). Letters a and b denote two independent replicates.

Minerals, Treatment	P of KH_2PO_4	Cu(II)	Fe(II)	Mn(II)	$Mn(IV)O_2$ [c]	Malate/Malon-Ate, mg L^{-1}	A_{420} of ABTS$^{\bullet+}$	$A_{520}-A_{561}$ of ABTS^{2+}	Single Absorbance Peaks
1a	Leach 263	0.050	0.049	0.013	0	0	BD, below detection	0.014 ± 0.007 up to 0.189	$A_{552}-A_{560}$
1b	Sum 1697 (+)	0.177 (+)	3.349 (+)	0.013 (−)	0 (−)	0 (−)	BD	0.044 ± 0.014	$A_{542}-A_{551}$
2a	263 (−)	0.177 (+)	3.349 (+)	55 (+)	690 (+)	7.7 (−)	0.780 (7 h)	0.108 ± 0.019	$A_{546}-A_{561}$
2b							0.214	0.114 ± 0.038	$A_{527}-A_{550}$
3a	263 (−)	0.177 (+)	3.349 (+)	55 (+)	690 (+)	679	0.999 (7 h)	0.071 ± 0.030	$A_{542}-A_{546}$
3b							0.416 (7 h)	0.057 ± 0.010	$A_{520}-A_{548}$
4b	1697 (+)	0.177 (+)	0.049 (-)	0.013 (−)	0 (−)	0 (−)	BD	0.024 ± 0.006	$A_{520}-A_{550}$
4b Lacc							0.311	0.444 ± 0.060	$A_{515}-A_{551}$
Rape	Leach rate, not determined (−)	>0.127 (+)	>3.30 (+)	>55 (+)	690 (+)	0 (−)	1.347 (30 h)	0.076 ± 0.013	A_{548}
Alfalfa							BD	0.248 ± 0.127	A_{543}

Time span denoting the drop of A_{420} absorbance values to (near) zero by reduction of the cation radical, followed by its partial transformation to ABTS^{2+} derivatives within ≤ 60 h. Unmarked absorbance values indicate stability of the green ABTS$^{\bullet+}$ solution for > 6 d of observation; (+), Minerals of the nutrient solution increased the pool of those leached from seeds; (−), in the current treatment, the modified nutrient solution did not contain these compounds; [c] MnO_2 oxide activated (Fluka) was applied to 2a, 3a, oilseed rape, and alfalfa. The less active MnO_2 powder (Merck) was applied to 2b and 3b.

3.2. Liquid Chromatography-Mass Spectrometry (LC-MS) Examination of a Non-Purified ABTS Derivative from White Mustard

Under the ionizing conditions of the weak acids in the eluent, the red ABTS derivative yielded major peaks at *m/z* 452.6 > 490.4 > 485.3. Among the numerous minor substances, *m/z* 514.1 to 514.2 represented the ABTS dianion molecule completed by two protons at the former NH_4 binding sites.

A derivative appearing at *m/z* 486.3 points to the replacement of two ethyl (C_2H_5) by methyl groups (CH_3) (Figure 3a,b).

(a)

(b)
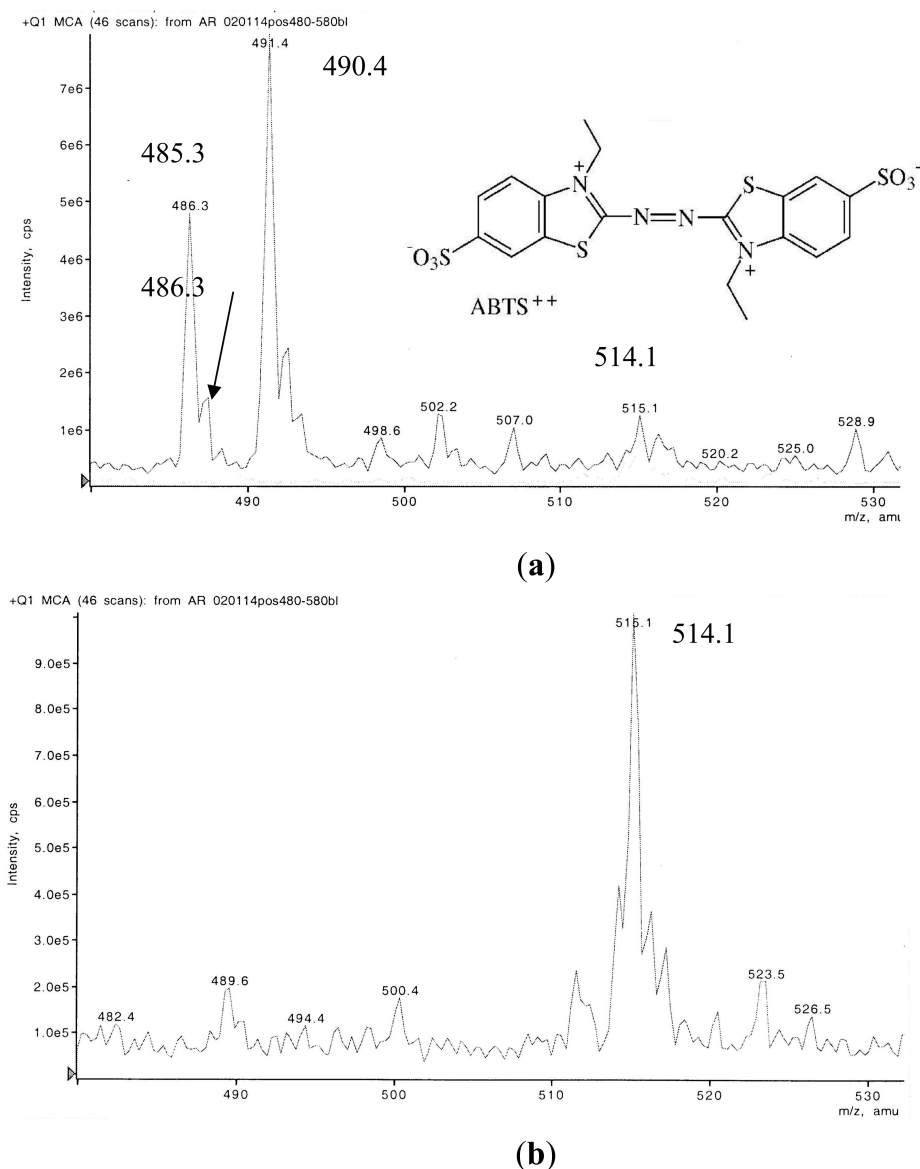
Figure 3. (**a**,**b**) Liquid-chromatography-mass spectrometry (LC-MS) chromatogram in the positive mode of a non-purified ABTS derivative with the protonated dianion of ABTS(2+) (*m/z* 514.1), its deethylated (C2H5) form recompleted by methyl groups (CH3, *m/z* 486.3), and major ABTS moieties.

Comparable disintegrations of the red ABTS^{2+} related product were also documented in preliminary Fourier-transform infrared spectrometry (FT-IR) analyses [62]. The lilac precipitates of a completely by $K_2O_8S_2$ oxidized monoazo compound of functional ABTS showed major stretching vibrations at 1506.6, 1472.8, and 1441.4 cm^{-1}. The range of (1555) 1525–1410 cm^{-1} is thereby associated with the presence of the -N=N- double bonds in the majority of azo dyes [63–66].

A soluble compound generated by fresh beech wood chips in the mode as above then showed the azo group related band at 1473.77 cm^{-1} in an environment of a general structural decay. Signals from P-O bonds around 859 cm^{-1} dominated [67].

3.3. Contributions of Abiotic Catalysts to the Oxidation of ABTS

The rate of ABTS oxidation by Fenton-like catalysts at pH 1.5–2 surpassed that in the physiological pH range of 3.8–6.0 drastically (Table 2). Moreover, the absence of KH_2PO_4 in the reaction mixture yielded higher A_{420} values and enabled the immediate production of red and insoluble $ABTS^{2+}$ products generated by two-electron oxidation (Figures 4 and 5). They are generally formed at pH around 2.0 in the presence of excess oxidant [16]. The insoluble compounds comproportionated to functional $ABTS^{\bullet+}$ by electron exchange with subsequently applied ABTS. Red compounds were not formed in the presence of buffer.

Table 2. Abiotic oxidation of ABTS to the green cation radical ($ABTS^{\bullet+}$) and to red $ABTS^{2+}$ products with absorbance peaks in the A_{482} to A_{601} range by active oxygen species alone or in combination with transition metal catalysts at physiological or suboptimal pH. Digits, temporary maximum absorbances A_{420} of $ABTS^{\bullet+}$ solutions.

Catalyst and Solvent	pH (2.3) 3.8–>6.0		pH 1.5–2.0	
	Water	KH_2PO_4 Buffer	Water	KH_2PO_4 Buffer
$O_2^{\bullet-}$ from KO_2	0 [a]	0	1.602 (6 days)	0.330
H_2O_2	0	0	1.604 (<4–5 h)	0.560
$MnSO_4/KO_2$	0	0	Insoluble red product $A_{482/529}$ [b]	1.165
$MnSO_4/H_2O_2$	0	0	1.636 (2.5–3 h)	0.620 (3 days)
$FeSO_4/KO_2$	0	0	0	0
$FeSO_4/H_2O_2$	0	0	0	0.395 (4 days)
$CuSO_4/KO_2$	0.252	0.650	1.276	0.744
$CuSO_4/H_2O_2$	0.816	0.506	1.115	0.511
$NiSO_4/KO_2$	0	0.021	1.748	0.738
$NiSO_4/H_2O_2$	0	0	1.804 (4 days)	0.180
$Pb(CH_3CO_2)_2/KO_2$	0	0.064	Insoluble red product $A_{553/601}$ [b]	0.813
$Pb(CH_3CO_2)_2/H_2O_2$	0.762	0	0.996	0.581
$CoCl_2/KO_2$	0.022	0.376	Insoluble red product $A_{514/596}$ [b]	0.950
$CoCl_2/H_2O_2$	0.384	Soluble red product A_{514} [b,c]	1.750 (1.5 h) [c]	1.182 (28 h) [c]

Time span denoting the drop of A_{420} absorbance values to (near) zero by reduction of the cation radical to the original ABTS. Unmarked absorbance values indicate stability of the green $ABTS^{\bullet+}$ solution for >6 d of observation. [a] No notable oxidative reaction; [b] Position of the absorbance peaks of the red $ABTS^{2+}$-related products; [c] The red solution of $CoCl_2$ peaking at $A_{511/512}$ may account for, or contribute to, the soluble red products of A_{514} that finally replace the green $ABTS^{\bullet+}$ stage.

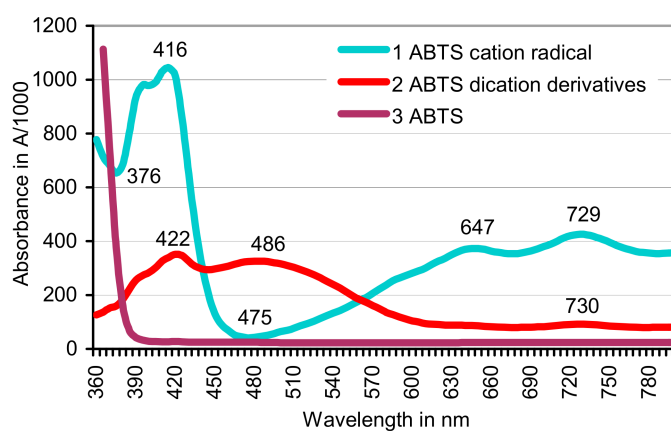**Figure 4.** Abiotic oxidation of ABTS by $MnSO_4/O_2^{\bullet-}$. Sample 1, in KH_2PO_4 buffer pH 1.7 to $ABTS^{\bullet+}$; sample 2, in water pH 1.7 to insoluble red $ABTS^{2+}$ moieties; sample 3, no oxidation in KH_2PO_4 buffer or water at pH 4.0.
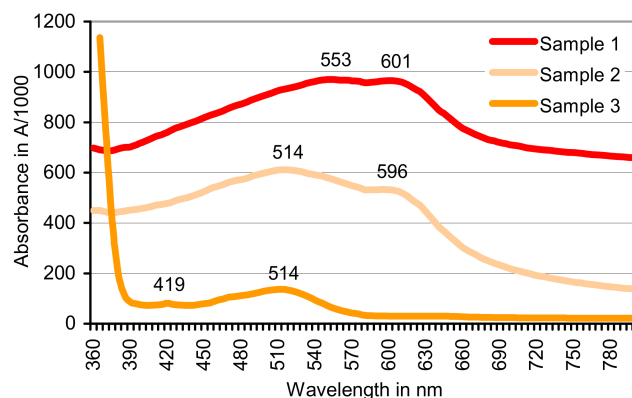
Figure 5. Abiotic oxidation of ABTS to red $ABTS^{2+}$ compounds by transition metal/active oxygen systems. Sample 1, by $Pb(CH_3CO_2)_2/O_2^{\bullet-}$ in water pH 2.2 to an insoluble product; sample 2, by $CoCl_2/O_2^{\bullet-}$ in water pH 1.7 to an insoluble product; sample 3, by $CoCl_2/H_2O_2$ in water pH 1.7 and KH_2PO_4 buffer at pH 4.0 to soluble products.

The insoluble red products generated by Co, Mn, and Pb catalysts in concert with KO_2 ($O_2^{\bullet-}$) displayed up to two absorbance peaks in the $ABTS^{2+}$-relevant 514-600 nm range (Figures 4 and 5). They corresponded with the insoluble $ABTS^{2+}$ compound formed by excess applications of $K_2O_8S_2$ oxidant at pH 2.15 with absorbance peaks at λ = 556 and 603 nm [16,62]. The soluble red product formed in three of four $CoCl_2/H_2O_2$ treatments peaking at A_{514} could be pretended, to the greatest extent, by the red color of the $CoCl_2$ itself with its single peak at A_{511} to A_{512}.

In general, abiotic contributions to the initial oxidation of ABTS at physiological pH could be expected from Co and Cu compounds in cooperation with $O_2^{\bullet-}$ and H_2O_2 both in water and KH_2PO_4 solution, and of Pb/H_2O_2 in water (Table 2). Combinations of Mn, Fe, and Ni alone with active oxygen were virtually inactive. Contemporarily, pH 1.5–2 conditions denoted by excess protons made the single active oxygen compounds $O_2^{\bullet-}$ and H_2O_2 as well as all metal/active oxygen combinations but those of Fe potent one-electron oxidants of ABTS. The reactions were somewhat less intense in the presence of KH_2PO_4 where white phosphate precipitates suggest binding of the transition metals. Low-pH disintegration of the ABTS itself did not seem to occur as its respective $ABTS^{\bullet+}$ lambda scans did not differ from those taken at physiological pH (Figure 4).

3.4. Interaction of Catalysts

The formation of red azodication derivatives from ABTS by aseptic plants is first evidence for their ability to initiate oxidative (chain) reactions with rhizosphere priming effects. As recently indicated, the stable and soluble azodication derivatives consist of $ABTS^{2+}$ molecules as a minority among lower-MW moieties with -N=N- double bonds (Figures 1 and 3a,b). They were generated by incubating PO-bearing sapwood chips of trees with ABTS and H_2O_2 in buffer solution. The catalysis of the initial green oxidation stage of $ABTS^{\bullet+}$ was ascribed to the PO/H_2O_2 system. The second oxidation step to $ABTS^{2+}$ only preceded with timber-released mediator molecules converted to radicals by $ABTS^{\bullet+}$ and possibly by the PO/H_2O_2 couple, too [62].

In this study, the outcome in red azodication derivatives was higher with PO-rich plants such as alfalfa and with supplements of fungal laccase and mineral catalysts such as MnO_2 that are independent of active oxygen species (Table 1). The spontaneous intense reddening of culture fluid aliquots amended with H_2O_2 and HRP showed that lacks in active oxygen and PO were the main limiting factors in a system containing enough root-exuded molecules that could act as catalysis-mediating aryloxy radicals.

The redox potential E^0 = 0.68 V for the oxidation of ABTS to $ABTS^{\bullet+}$ is in the range of plant PO (E^0 = 0.89–0.95 V) [18] and Mn^{3+} (0.8–0.9V) [20,21] formed from Mn(II) by PO-catalyzed aryloxy radicals [15,32]. Accordingly, Mn(II) starvation in the treatments 1a, 1b, and 4b led to the lowest outcome in azodication production (Table 1) but possibly, too, in a drop of enzyme release that is

stimulated by mineral fertilizing [37]. Contributions of root-exuded laccase (E^0 = 0.4 V) and MMO (E^0 = 0.26 V) traces as active oxygen independent enzymes may solely depend on proper redox mediator systems to overcome their deficit in redox potential. The oxidation of ABTS by pyrolusite (MnO_2) as a member of oxygen neutral clay minerals [45] may obey the rule upon the formation of manganite, with Mn being in the three-valent stage as a consequence of a transient H^+/e^- incorporation [68,69].

$$Mn(IV)O_2 + ABTS + H^+ \rightarrow Mn(III)OOH + ABTS^{\bullet+} \tag{3}$$

Pyrolusite in plant-soil systems was mainly regarded as a source of Mn^{3+} released from the mineral by root-exuded carboxylate chelants [55]. Actually, P and Fe(II) starvation increased malate/malonate release and may have contributed, as underpinned by further exogenous malate supply, to higher ABTS transformation rates. It is known that Mn^{3+} initiated, too, the degradation of malonate to formate at least in the presence of MnP and yielded $O_2^{\bullet-}$, H_2O_2, and acetate radical ($COOH\text{-}CH_2^{\bullet}$) catalysts [70]. In reactions of $O_2^{\bullet-}$ with metal cations, Mn^{3+} or $HO^{\bullet}$ [71] are formed:

$$O_2^{\bullet-} + Mn^{2+} + 2\,H^+ \rightarrow Mn^{3+} + H_2O_2 \tag{4}$$

$$O_2^{\bullet-} + Fe^{2+} + 2\,H^+ \rightarrow Fe^{3+} + H_2O_2 \tag{5}$$

$$O_2^{\bullet-} + Fe^{3+} \rightarrow O_2 + Fe^{2+} \tag{6}$$

$$Fe^{2+} + H_2O_2 \rightarrow Fe^{3+} + HO^- + HO^{\bullet} \text{ (Fenton reaction)} \tag{7}$$

$$O_2^{\bullet-} + H_2O_2 \rightarrow HO^- + HO^{\bullet} + O_2 \text{ (Haber-Weiss reaction)} \tag{8}$$

The transition metals Co, Cu, Fe, Mn, Ni, (and Pb) released from the plants and supplied, in part, with the nutrient solution formed therefore the ultimate oxidant $HO^{\bullet}$ (E^0 = 1.8–2.7 V) in a Fenton–like reaction (see Equation (2)) [40,41] both with $O_2^{\bullet-}$ and H_2O_2. As indicated by the conversion of ABTS, the high rate of hydroxyl radical formation at pH 1.5–2 dropped to a moderate level at the physiological pH of the plant cultures in the reaction with Co, Cu, and Pb, whereas Fe and Mn failed to cooperate (Table 2).

Contemplating the treatments 1a and 4b with Cu(II) as the only efficient Fenton metal (Table 1), it is concluded that plants initiate oxidative activities in the rhizosphere by the release of peroxidases, carboxylates, and occasional traces of active oxygen species at least in alfalfa [38]. Azodication derivatives in the culture fluids confirm the presence of root–released phenolic molecules, too, that had been oxidized to aryloxy radicals with the respective redox mediator potential [62]. Their formation could mainly be ascribed to the PO/active–oxygen couple but also to the by–production of Mn^{3+} with the aid of the radicals in turn. In the absence of external H_2O_2, POs generate it by themselves from electron donors such as the intracellular NAD(P)H, indole-3-acetic acid, thiols (glutathione), and carboxylates [15,33,70]. Oxidative contributions of $HO^{\bullet}$ generated by Cu(I)/Cu(II) in a Fenton–like reaction with $O_2^{\bullet-}$ and H_2O_2 may be less efficient. Cu(I) mainly reacts with O_2 without the production of the hydroxyl radical [42]. In contrast, active oxygen independent catalysts such as pyrolusite, laccase, and Mn^{3+}/malate complexes like the excessive release of alfalfa PO increased the efficacy of ABTS oxidation. The results encourage further studies into the control of micropollutants such as agrochemicals, pharmaceuticals, and endocrine disrupting compounds in soil by PO releasing crops.

References

1. Hedges, J.I.; Eglinton, G.; Hatcher, P.G.; Kirchman, D.L.; Arnosti, C.; Derenne, S.; Evershed, R.P.; Kögel-Knabner, I.; De Leeuw, J.W.; Littke, R.; et al. The molecularly uncharacterized component of nonliving organic matter in natural environments. *Org. Geochem.* **2000**, *31*, 945–958. [CrossRef]

2. Kuzyakov, Y. Priming effects: interactions between living and dead organic matter. *Soil Biol. Biochem.* **2010**, *42*, 1363–1371. [CrossRef]

3. Fu, S.; Cheng, W. Rhizosphere priming effects on the decomposition of soil organic matter in C4 and C3 grassland soils. *Plant Soil* **2002**, *238*, 289–294. [CrossRef]

4. Haider, K.; Heinemeyer, O.; Mosier, A.R. Effects of growing plants on humus and plant residue decomposition in soil; uptake of decomposition products by plants. *Sci. Total Environ.* **1989**, *81/82*, 661–670. [CrossRef]

5. Dijkstra, F.A.; Cheng, W.X.; Johnson, D.W. Plant biomass influences rhizosphere priming effects on soil organic matter decomposition in two differently managed soils. *Soil Biol. Biochem.* **2006**, *38*, 2519–2526. [CrossRef]

6. Zhu, B.; Cheng, W.X. Nodulated soybean enhances rhizosphere priming effects on soil organic matter decomposition more than nonnodulated soybean. *Soil Biol. Biochem.* **2012**, *51*, 56–65. [CrossRef]

7. Zhu, B.; Gutknecht, J.L.M.; Herman, D.J.; Keck, D.C.; Firestone, M.K.; Cheng, W. Rhizosphere priming effects on soil carbon and nitrogen mineralization. *Soil Biol. Biochem.* **2014**, *76*, 183–192. [CrossRef]

8. Bringezu, S.; Schütz, H.; Pengue, W.; O'Brien, M.; Garcia, F.; Sims, R.; Howarth, R.W.; Kauppi, L.; Swilling, M.; Herrick, J. *Assessing Global Land Use: Balancing Consumption with Sustainable Supply. A Report of the Working Group on Land and Soils of the International Resource Panel*; United Nations Environment Programme: Nairobi, Kenya, 2014; ISBN 978-92-807-3330-3.

9. Arora, D.S.; Sharma, R.K. Ligninolytic fungal laccases and their biotechnological applications. *Appl. Biochem. Biotechnol.* **2010**, *160*, 1760–1788. [CrossRef] [PubMed]

10. Burns, R.G.; DeForest, J.L.; Marxsen, J.; Sinsabaugh, R.L.; Stromberger, M.E.; Wallenstein, M.D.; Weintraub, M.N.; Zoppini, A. Soil enzymes in a changing environment: Current knowledge and future directions. *Soil Biol. Biochem.* **2013**, *58*, 216–234. [CrossRef]

11. Kirk, T.K.; Farrell, R.L. Enzymatic "combustion": The microbial degradation of lignin. *Annu. Rev. Microbiol.* **1987**, *41*, 465–505. [CrossRef] [PubMed]

12. Wang, L.; Nie, Y.; Tang, Y.Q.; Song, X.M.; Cao, K.; Sun, L.Z.; Wang, Z.-J.; Wu, X.-L. Diverse bacteria with lignin degrading potentials isolated from two ranks of coal. *Front. Microbiol.* **2016**, *7*, 1428. [CrossRef] [PubMed]

13. Husain, Q. Peroxidase mediated decolorization and remediation of wastewater containing industrial dyes: a review. *Rev. Environ. Sci. Biotechnol.* **2010**, *9*, 117–140. [CrossRef]

14. Eggert, C.; Temp, U.; Dean, J.F.D.; Eriksson, K.E.L. A fungal metabolite mediates degradation of non-phenolic lignin structures and synthetic lignin by laccase. *FEBS Lett.* **1996**, *391*, 144–148. [CrossRef]

15. Gramss, G. Potential contributions of oxidoreductases from alfalfa plants to soil enzymology and biotechnology: A review. *J. Nat. Sci. Sustain. Technol. (Nova)* **2012**, *6*, 169–223.

16. Johannes, C.; Majcherczyk, A. Natural mediators in the oxidation of polycyclic aromatic hydrocarbons by laccase mediator systems. *Appl. Environ. Microbiol.* **2000**, *66*, 524–528. [CrossRef] [PubMed]

17. Torres, C.E.; Negro, C.; Fuente, E.; Blanco, A. Enzymatic approaches in paper industry for pulp refining and biofilm control. *Appl. Microbiol. Biotechnol.* **2012**, *96*, 327–344. [CrossRef] [PubMed]

18. Ayala, M.; Roman, R.; Vazquez-Duhalt, R. A catalytic approach to estimate the redox potential of heme-peroxidases. *Biochem. Biophys. Res. Commun.* **2007**, *357*, 804–808. [CrossRef] [PubMed]

19. Hofrichter, M.; Ullrich, R.; Pecyna, M.J.; Liers, C.; Lundell, T. New and classic families of secreted fungal heme peroxidases. *Appl. Microbiol. Biotechnol.* **2010**, *87*, 871–897. [CrossRef] [PubMed]

20. Wong, D.W.S. Structure and action mechanism of ligninolytic enzymes. *Appl. Biochem. Biotechnol.* **2009**, *157*, 174–209. [CrossRef] [PubMed]

21. Cui, F.; Dolphin, D. The role of manganese in model systems related to lignin biodegradation. *Holzforschung* **1990**, *44*, 279–283. [CrossRef]

22. Hammel, K.E.; Jensen, K.A., Jr.; Mozuch, M.D.; Landucci, L.L.; Tien, M.; Pease, E.A. Ligninolysis by a purified lignin peroxidase. *J. Biol. Chem.* **1993**, *268*, 12274–12281. [PubMed]

23. Nousiainen, P.; Kontro, J.; Manner, H.; Hatakka, A.; Sipila, J. Phenolic mediators enhance the manganese peroxidase catalyzed oxidation of recalcitrant lignin model compounds and synthetic lignin. *Fung. Gen. Biol.* **2014**, *72*, 137–149. [CrossRef] [PubMed]

24. Kersten, P.J.; Kalyanaraman, B.; Hammel, K.E.; Reinhammar, B. Comparison of lignin peroxidase, horseradish peroxidase and laccase in the oxidation of methoxybenzenes. *Biochem. J.* **1990**, *268*, 475–480. [CrossRef] [PubMed]

25. Kawai, S.; Umezawa, T.; Higuchi, T. Degradation mechanisms of phenolic β-1 lignin substructure model compounds by laccase of *Coriolus versicolor*. *Arch. Biochem. Biophys.* **1988**, *262*, 99–110. [CrossRef]

26. Kawai, S.; Umezawa, T.; Shimada, M.; Higuchi, T. Aromatic ring cleavage of 4,6-di(*tert*-butyl) guaiacol, a phenolic lignin model compound, by laccase of *Coriolus versicolor*. *FEBS Lett.* **1988**, *236*, 309–311. [CrossRef]

27. Bourbonnais, R.; Leech, D.; Paice, M.G. Electrochemical analysis of the interactions of laccase mediators with lignin model compounds. *Biochim. Biophys. Acta* **1998**, *1379*, 381–390. [CrossRef]

28. Branchi, B.; Galli, C.; Gentili, P. Kinetics of oxidation of benzyl alcohols by the dication and radical cation of ABTS. Comparison with laccase-ABTS oxidations: An apparent paradox. *Org. Biomol. Chem.* **2005**, *3*, 2604–2614. [CrossRef] [PubMed]

29. Brijwani, K.; Rigdon, A.; Vadlani, P.V. Fungal laccases: Production, function, and applications in food processing. *Enzym. Res. (Hindawi)* **2010**. [CrossRef] [PubMed]

30. Gramss, G.; Günther, Th.; Voigt, K.-D.; Kirsche, B. Comparative activities of oxidoreductase enzymes in tissue extracts of crop plants and in culture fluids of fungal mycelia. *Chemosphere* **1998**, *36*, 1923–1934. [CrossRef]

31. Gramss, G.; Ziegenhagen, D.; Sorge, S. Degradation of soil humic extract by wood- and soil-associated fungi, bacteria, and commercial enzymes. *Microb. Ecol.* **1999**, *37*, 140–151. [CrossRef] [PubMed]

32. Kenten, R.H.; Mann, P.J.G. The oxidation of manganese by peroxidase systems. *Biochem. J.* **1950**, *46*, 67–73. [CrossRef] [PubMed]

33. Siegel, B.Z. Plant peroxidases—An organismic perspective. *Plant Growth Regul.* **1993**, *12*, 303–312. [CrossRef]

34. Dean, J.F.D.; Eriksson, K.-E.L. Laccase and the deposition of lignin in vascular plants. *Holzforschung* **1994**, *48*, 21–33. [CrossRef]

35. Lee, T.-M.; Lin, Y.-H. Changes in soluble and cell wall-bound peroxidase activities with growth in anoxia-treated rice (*Oryza sativa* L.) coleoptiles and roots. *Plant Sci.* **1995**, *106*, 1–7. [CrossRef]

36. Muratova, A.; Pozdnyakova, N.; Golubev, S.; Wittenmayer, L.; Makarov, O.; Merbach, W.; Turkovskaya, O. Oxidoreductase activity of sorghum root exudates in a phenanthrene-contaminated environment. *Chemosphere* **2009**, *74*, 1031–1036. [CrossRef] [PubMed]

37. Gramss, G.; Voigt, K.-D.; Kirsche, B. Oxidoreductase enzymes liberated by plant roots and their effects on soil humic material. *Chemosphere* **1999**, *38*, 1481–1494. [CrossRef]

38. Gramss, G.; Rudeschko, O. Activities of oxidoreductase enzymes in tissue extracts and sterile root exudates of three crop plants, and some properties of the peroxidase component. *New Phytol.* **1998**, *138*, 401–409. [CrossRef]

39. Mahro, B.; Kästner, M. The microbial degradation of polycyclic aromatic hydrocarbons in soil and sediments: Mineralization, metabolite excretion and the formation of bound residues. *BioEngineering* **1993**, *9*, 50–58.

40. Huang, K.-C.; Couttenye, R.A.; Hoag, G.E. Kinetcs of heat-assisted persulfate oxidation of methyl tert-butyl ether (MTBE). *Chemosphere* **2002**, *49*, 413–420. [CrossRef]

41. Haber, F.; Weiss, J. The catalytic decomposition of hydrogen peroxide by iron salts. *Proc. R. Soc. A* **1934**, *147*, 332–351. [CrossRef]

42. Bokare, A.D.; Choi, W. Review of iron-free Fenton-like systems for activating H_2O_2 in advanced oxidation processes. *J. Hazard. Mater.* **2014**, *275*, 121–135. [CrossRef] [PubMed]

43. Barbusiński, K. Fenton reaction–controversy concerning the chemistry. *Ecol. Chem. Eng. S* **2009**, *16*, 347–358.

44. Chumakov, A.; Batalova, V.; Slizhov, Y. Electro-Fenton-like reactions of transition metal ions with electrogenerated hydrogen peroxide. In *Prospects of Fundamental Sciences Development (PFSD-2016)*; AIP Publishing: New York, NY, USA, 2016; Volume 1772, pp. 040004-1–040004-6. ISBN 978-0-7354-1430-3.

45. Garrido-Ramírez, E.G.; Theng, B.K.G.; Mora, M.L. Clays and oxide minerals as catalysts and nanocatalysts in Fenton-like reactions—A review. *Appl. Clay Sci.* **2010**, *47*, 182–192. [CrossRef]

46. Susic, M. Replenishing humic acids in agricultural soils. *Agronomy* **2016**, *6*, 45. [CrossRef]

47. Schachtschabel, P.; Blume, H.-P.; Brümmer, G.; Hartge, K.H.; Schwertmann, U. *Lehrbuch der Bodenkunde*, 14th ed.; Enke: Stuttgart, Germany, 1998.

48. Stevenson, F.J. *Humus Chemistry*, 2nd ed.; John Wiley & Sons: New York, NY, USA, 1994.

49. Grinhut, T.; Salame, T.M.; Chen, Y.; Hadar, Y. Involvement of ligninolytic enzymes and Fenton-like reaction in humic acid degradation by *Trametes* sp. *Appl. Microbiol. Biotechnol.* **2011**, *91*, 1131–1140. [CrossRef] [PubMed]

50. Solarska, S.; May, T.; Roddick, F.A.; Lawrie, A.C. Isolation and screening of natural organic matter-degrading fungi. *Chemosphere* **2009**, *75*, 751–758. [CrossRef] [PubMed]

51. Steffen, K.T.; Hatakka, A.; Hofrichter, M. Degradation of humic acids by the litter-decomposing basidiomycete *Collybia dryophila*. *Appl. Environ. Microbiol.* **2002**, *68*, 3442–3448. [CrossRef] [PubMed]

52. Wackett, L.P.; Gibson, D.T. Rapid method for detection and quantitation of hydroxylated aromatic intermediates produced by microorganisms. *Appl. Environ. Microbiol.* **1983**, *45*, 1144–1147. [PubMed]

53. Yuan, Y.; Zhao, W.; Xiao, J.; Zhang, Z.; Qiao, M.; Liu, Q.; Yin, H. Exudate components exert different influences on microbially mediated C losses in simulated rhizosphere soils of a spruce plantation. *Plant Soil* **2017**, *419*, 127–140. [CrossRef]

54. Hofrichter, M.; Scheibner, K.; Schneegass, I.; Ziegenhagen, D.; Fritsche, W. Mineralization of synthetic humic substances by manganese peroxidase from the white-rot fungus *Nematoloma frowardii*. *Appl. Microbiol. Biotechnol.* **1998**, *49*, 584–588. [CrossRef]

55. Godo, G.H.; Reisenauer, H.M. Plant effects on soil manganese availability. *Soil Sci. Soc. Am. J.* **1980**, *44*, 993–995. [CrossRef]

56. Scott, S.L.; Chen, W.-J.; Jjakac, A.; Espenson, J.H. Spectroscopic parameters, electrode potentials, acid ionization constants, and electron exchange rates of the 2,2′-azinobis(3-ethylbenzothiazoline-6-sulfonate) radicals and ions. *J. Phys. Chem.* **1993**, *97*, 6710–6714. [CrossRef]

57. Fries, N. Spontaneous physiological mutations in *Ophiostoma*. *Hereditas* **1948**, *34*, 338–350. [CrossRef]

58. Wariishi, H.; Valli, K.; Renganathan, V.; Gold, M.H. Thiol-mediated oxidation of nonphenolic lignin model compounds by manganese peroxidase of *Phanerochaete chrysosporium*. *J. Biol. Chem.* **1989**, *264*, 14185–14191. [PubMed]

59. Sterjiades, R.; Dean, J.F.D.; Eriksson, K.-E.L. Laccase from sycamore maple (*Acer pseudoplatanus*) polymerizes monolignols. *Plant Physiol.* **1992**, *99*, 1162–1168. [CrossRef] [PubMed]

60. Givaudan, A.; Effose, A.; Faure, D.; Portier, P.; Bouillant, M.-L.; Bally, R. Phenol oxidase in *Azospirillum lipoferum* isolated from rice rhizosphere: Evidence for laccase activity in non-motile strains of *Azospirillum lipoferum*. *FEMS Microbiol. Lett.* **1993**, *108*, 205–210.

61. Gramss, G.; Voigt, K.-D. Regulation of the mineral concentrations in pea seeds from uranium mine and reference soils diverging extremely in their heavy metal load. *Sci. Hort.* **2015**, *194*, 255–266. [CrossRef]

62. Gramss, G. Reappraising a controversy: Formation and role of the azodication (ABTS[2+]) in the laccase-ABTS catalyzed breakdown of lignin. *Fermentation* **2017**, *3*, 27. [CrossRef]

63. Ahmed, F.; Dewani, R.; Pervez, M.K.; Mahboob, S.J.; Soomro, S.A. Non-destructive FT-IR analysis of mono azo dyes. *Bulgar. Chem. Commun.* **2016**, *48*, 71–77.

64. Awale, A.G.; Gholse, S.B.; Utale, P.S. Synthesis, spectral properties and applications of some mordant and disperse mono azo dyes derived from 2-amino-1,3-benzothiazole. *Res. J. Chem. Sci.* **2013**, *3*, 81–87.

65. Dinçalp, H.; Toker, F.; Durucasu, I.; Avcıbaşı, N.; Icli, S. New thiophene-based azo ligands containing azo methine group in the main chain for the determination of copper(II) ions. *Dyes Pigments* **2007**, *75*, 11–24. [CrossRef]

66. Masoud, M.S.; Khalil, E.A.; Hindawya, A.M.; Ali, A.E.; Mohamed, E.F. Spectroscopic studies on some azo compounds and their cobalt, copper and nickel complexes. *Spectrochim. Acta A* **2004**, *60*, 2807–2817. [CrossRef] [PubMed]

67. Yuen, C.W.M.; Ku, S.K.A.; Choi, P.S.R.; Kan, C.W.; Tsang, S.Y. Determining functional groups of commercially available ink-jet printing reactive dyes using Infrared Spectroscopy. *RJTA* **2005**, *9*, 26–38. [CrossRef]

68. Toupin, M.; Brousse, T.; Bélanger, D. Charge storage mechanism of MnO_2 electrode used in aqueous electrochemical capacitor. *Chem. Mater.* **2004**, *16*, 3184–3190. [CrossRef]

69. Wang, Y.; Stone, A.T. Reaction of MnIII,IV (hydr)oxides with oxalic acid, glyoxylic acid, phosphonoformic acid, and structurally-related organic compounds. *Geochim. Cosmochim. Acta* **2006**, *70*, 4477–4490. [CrossRef]

70. Hofrichter, M.; Ziegenhagen, D.; Vares, T.; Friedrich, M.; Jäger, M.G.; Fritsche, W.; Hatakka, A. Oxidative decomposition of malonic acid as basis for the action of manganese peroxidase in the absence of hydrogen peroxide. *FEBS Lett.* **1998**, *434*, 362–366. [CrossRef]

71. Koppenol, W.H.; Liebman, J.F. The oxidizing nature of the hydroxyl radical. A comparison with the ferryl ion (Fe0^{2+}). *J. Phys. Chem.* **1984**, *88*, 99–101. [CrossRef]